

Investigation of Carbon Allotropes for Simultaneous Determination of Ascorbic Acid, Epinephrine, Uric Acid, Nitrite and Xanthine

Masoumeh Tohidinia, Meissam Noroozifar*

Department of Chemistry, University of Sistan and Baluchestan, Zahedan, P.O. Box 98135-674, Iran

*E-mail: mnoroozifar@chem.usb.ac.ir

Received: 2 October 2017 / Accepted: 23 December 2017 / Published: 5 February 2018

In this study, modified glassy carbon electrode (GCE) with different carbon allotropes such as multiwall carbon nanotubes (MWCNTs), graphene, bucky ball and graphite have been used for the simultaneous determination of ascorbic acid (AA), epinephrine (EP), uric acid (UA), Nitrite (NO_2^-), and xanthine (XN). Different electrochemical methods such as cyclic voltammetry, differential pulse voltammetry and chronoamperometry methods were employed to study the behavior of AA, EP, UA, NO_2^- and XN on these proposed modified electrodes. The modified GCE with MWCNTs was successfully used for simultaneous determination of AA, EP, UA, NO_2^- and XN. The electron transfer coefficients, diffusion coefficients and standard heterogeneous rate constant were determined for the electrochemical oxidation of AA, EP, UA, NO_2^- and XN. Under the optimum conditions, detection limits of 16.3, 3.92, 0.37, 29.9 and 0.13 μM were obtained for AA, EP, UA, NO_2^- , and XN, respectively. Moreover, the best modified GCE was applied for simultaneous determination of AA, EP, UA, NO_2^- , and XN in Human urine, serum and AA Tables samples.

Keywords: Carbon allotropes, Simultaneous determination, Bio-compounds, Nitrite.

1. INTRODUCTION

Allotropy is the different physical forms of the similar element that exist in two or more different physical forms. All elements are made up uniquely of their own atoms and hence any physical differences must be a result of how the atoms are joined together [1]. In the case of carbon, the atoms of carbon can be bonded with different ways with each other's, termed allotropes of carbon such as graphite (G), diamond, graphene (GP), carbon nanotubes (CNTs) and bucky-ball (BB) due to the ability to form sp , sp^2 , and sp^3 bonds. For example, a single layer of graphite is called graphene [2] with sp^2 orbital hybridization. These carbon allotropes have been shown different physical properties. For examples in diamond the carbons in the mass structure are joined together by covalent bonds

making attach molecules and diamond is the hardest material [3] while graphite is soft enough to form a streak on paper or in case BB, there is only separate molecules made up of 60 carbons in a structure resembling a ball shapes [4]. The CNTs is a cylindrical form allotrope of carbon with subdivided into single and multi-walled CNTs (MWCNTs). CNTs have an sp^2 bond between carbon atoms such as G [5]. The carbon allotropes with different bond types reveal distinct electrical, thermal, and physical properties. G, GP, CNTs and BB have different conductivity and shapes that can be used in electrochemistry studies.

Ascorbic acid (AA) also called vitamin C is a fundamental vitamin present as an anti-oxidant in many biological systems for the treatment of the common mental illness and in the absorption of iron in hemoglobin as well as for the debarment and therapy infertility, cancers, and AIDS [6-9]. Epinephrine (EP) is a momentous catecholamine neurotransmitter in the mammalian central nerves system and the changes EP concentration is important [6, 10, 11]. Uric acid (UA) is product of purine metabolism, inordinate level of UA in the body is symptoms of several diseases like gout, hyperuricaemia, etc. [6, 12]. Nitrite (NO_2^-) effects on blood pressure and blood flow and the nitrite test of urine has been used as a rapid screening test for significant bacteriuria [13, 14]. Xanthine (XN) is in purine metabolism as an intermediate and found in most human body tissues and fluids and in other organisms [15, 16]. XN is the first indicator of an unusual purine profile, and can serve as a marker of sharp hypoxia stress, cerebral ischemia and pre-eclampsia. Since designation of XN in serum/urine is very serious in the assessment and medical management of hyperuricemia, gout, xanthinuria and renal failure. The value of XN in the blood and the tissue samples should be easily analyzed for the assessment and the treatment of various diseases [16-20]. Today, clinical laboratories perform a lot testing for determination of these analytes in the real samples such as human blood serum and urine. Simultaneous measurement of these compounds in the biological samples is great to decrease the analysis time and lower costs. In other hand, the simultaneous determination of the AA, EP, UA, NO_2^- and XN are very important because they co-exist in human biological fluids.

In the present study, four famous allotropes of carbons G, GP, MWCNTs and BB were used as modifiers and chitosan (CH) as binder for modification of glassy carbon electrodes (GCE). The electrochemical behaviors of different modified electrodes were investigated for simultaneous measurement of AA, EP, UA, NO_2^- and XN. There is no report for comparison study of these modified electrodes for simultaneous determination of AA, EP, UA, NO_2^- and XN. Based on these results, pH 2 exhibits the best peak separation and highest peak current for the GCE/MWCNTs-CH. The proposed method can be applied to the determination of AA, EP, UA, NO_2^- and XN in real samples with satisfactory results.

2. EXPERIMENTAL

2.1. Reagents

MWCNTs with diameters $OD = 20-30$ nm, wall thickness = 1–2 nm, length = 0.5–2 μ m and purity > 95%, and BB, as produced cylinders, chitosan (CH) (medium molecular weight) as binder, AA, EP, UA, XN and NO_2^- were purchased from Sigma-Aldrich Company. GP was purchased from US Nano Research. High purity G powder, potassium chloride, sodium hydroxide, potassium

ferrocyanide, potassium ferricyanide, phosphoric acid and sulfuric acid were purchased from Merck Company. The stock solutions of AA (0.1 M), EP (0.01 M) and NO_2^- (0.1M) were daily prepared by dissolving AA, EP and NO_2^- in doubly distilled water (DDW). The stock solution of UA (0.01 M) and XN (0.01M) were prepared by dissolving the solid in a small volume of 0.1 M NaOH solution then diluted to reach final concentration. Phosphate buffer solutions (PBS) were prepared from H_3PO_4 (0.1 M); we adjusted the pH range to 2.0 – 7.0 with 0.1 M H_3PO_4 and NaOH. All solutions were prepared with doubly distilled water. Fresh serum and urine samples were obtained from the Mehran Clinical Laboratory (Zahedan, Iran) without any pretreatments.

2.2. Apparatus

Electrochemical measurements were performed with an SAMA-500 electro analyzer (SAMA Research Center, Iran) controlled by a personal computer. All electrochemical experiments were carried out in a conventional three-electrode cell at room temperature. A glassy carbon electrode (GCE), a platinum electrode and a silver chloride (Ag/AgCl) electrode were used as the working, counter and reference electrodes, respectively. Electrochemical impedance spectroscopy (ESI) was performed with an Autolab PGSTAT 128N (Eco Chemie, Netherlands) potentiostat/galvanostat controlled by NOVA 1.11 software. ESI were performed in 5 mM $[\text{Fe}(\text{CN})_6]^{3-/4-}$ prepared in 0.1 M KCl. EIS was performed over a frequency range of 0.01 Hz to 100 kHz with 0.02 V amplitude (rms). Transmission electron microscopy (TEM) images were taken using a Philips CM120 transmission electron microscopy with 2.5 Å resolutions. Ultrasonic 4D Euronda brands were used. A Metrohm pH meter, model 744 was also used for pH measurements.

2.3. Preparation of modified electrodes

The GCEs were polished with 0.05 μm alumina slurry until mirror like surface were achieved. The GCE further was cleaned and activated for generating anchoring sites on its surface by using cyclic voltammetry in the potential range of -1.5 to 1.5 V of a 1 M H_2SO_4 solution with a scan rate 100 mVs^{-1} (≈ 15 cycles). 5 mg of each carbon allotropies in 2.5 ml of the double distilled water (DDW) was mixed with 2.5 ml of the CH solution (1 % w/v) and then sonicated for 1 h. 5 μl of this suspension for each carbon allotropies were dripped by a micropipette on the GCEs surface and then dried at 60 $^\circ\text{C}$ for 1 h. These modified electrodes were denoted as GCE/MWCNTs-CH, GCE/GP-CH, GCE/BB-CH and GCE/G-CH. The GCE/CH was prepared with the same method without modifier.

3. RESULT AND DISCUSSION

3.1. TEM characterization of electrodes

The morphology of different electrodes structures was characterized by transmission electron microscopy (TEM). Fig. 1 shows TEM images of MWCNTs-CH, GP-CH, BB-CH and G-CH.

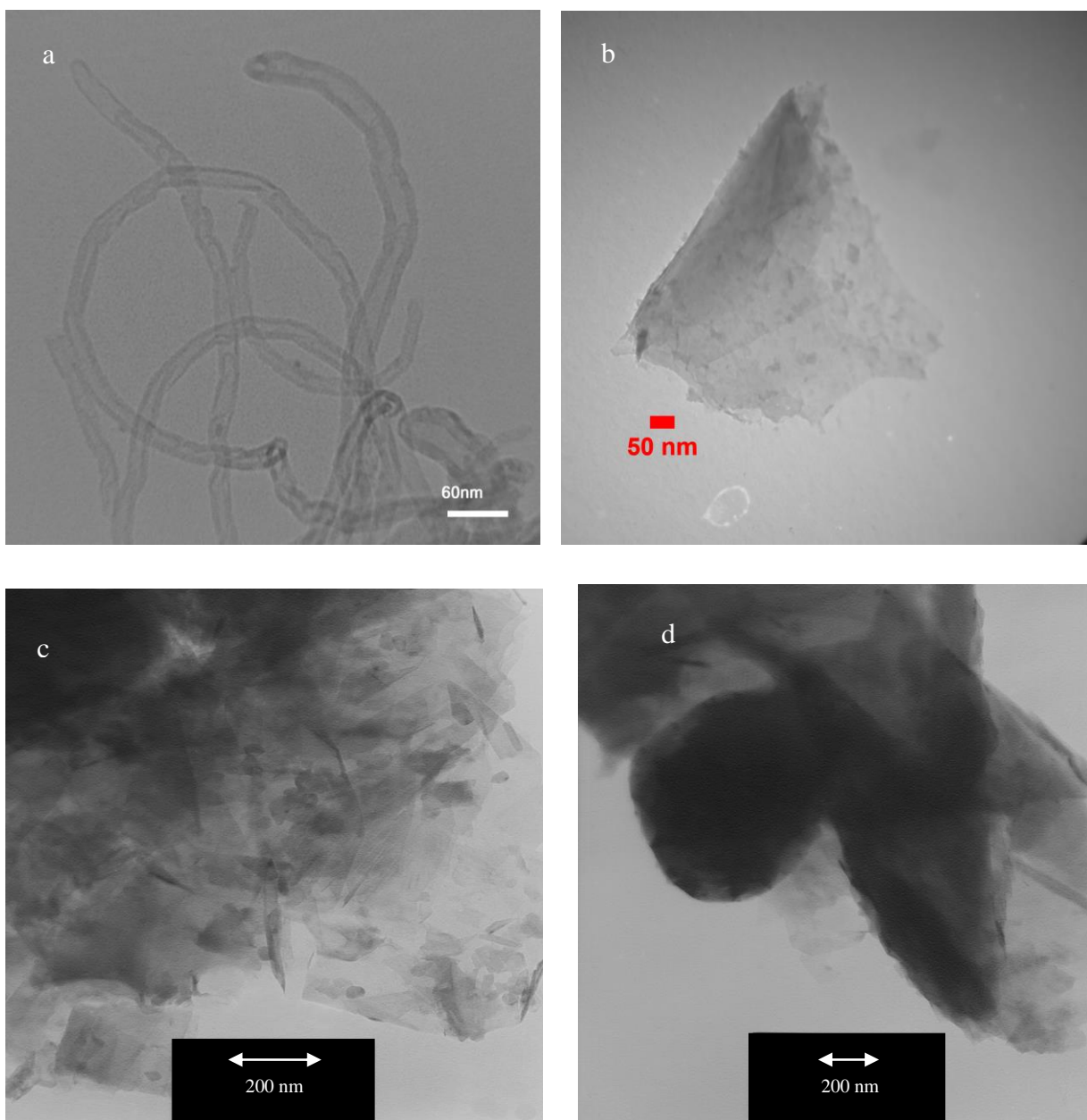


Figure 1. TEM images of (a) CNTs (b) GP (c) BB (d) G.

Based on these Figures, the MWCNTs and GP are not aggregate in presence of CH. It means that CH can interact with MWCNT, GP and makes heavily entangled them from finer bundles.

3.2. EIS Measurements

Fig. 2A shows the cyclic voltammeters (CVs) of 5 mM $\text{Fe}(\text{CN})_6^{3-/4-}$ in 0.1 M KCl at various electrodes. It was found that the modification of bare GCE result in remarkable decrease in ΔE_p and remarkable increase in peak current and the modification of electrode from GCE/MWCNTs-CH, GCE/GP-CH, GCE/BB-CH, GCE/G-CH and GCE/CH exhibits decrease in peak current. For the purpose of further study of electrodes surface features the EIS was utilized.

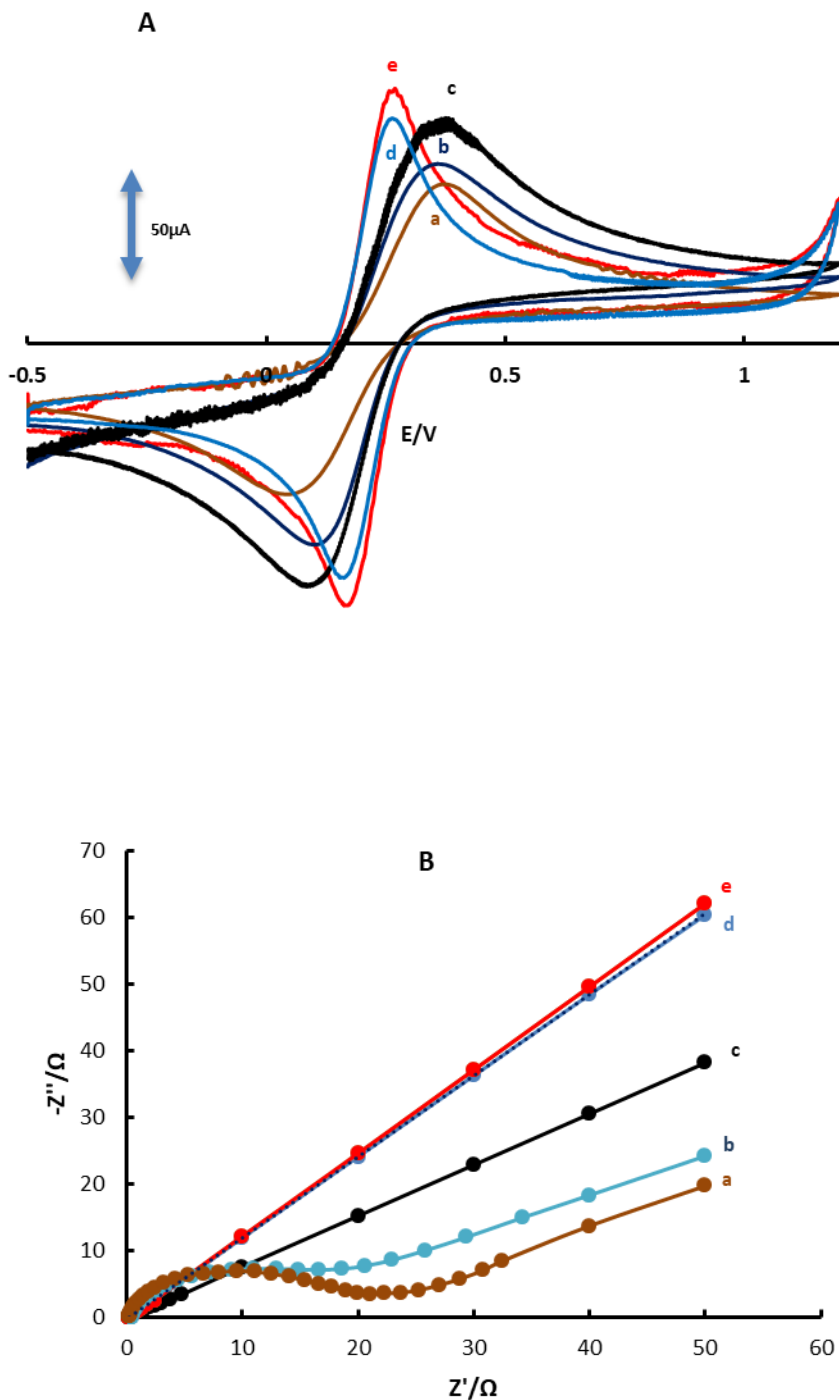


Figure 2. (A) CVs of (a) GCE/CH (b) GCE/G-CH (c) GCE/BB-CH (d) GCE/GP-CH and (e) GCE/MWCNTs/CH in 5 mM $[\text{Fe}(\text{CN})_6]^{3-/4-}$ prepared in 0.1 M KCl. (B) Nyquist plots showing the step-wise modification of (a) GCE/CH (b) GCE/G-CH (c) GCE/BB-CH (d) GCE/GP-CH and (e) GCE/MWCNTs/CH. Electrochemical measurements were performed in 5 mM $[\text{Fe}(\text{CN})_6]^{3-/4-}$ prepared in 0.1 M KCl. EIS was analyzed over a frequency range of 0.1 Hz to 10 kHz.

As shown in Fig. 2B, the Nyquist plot of GCE/G-CH and GCE/CH comprises two parts, one semicircle at higher frequencies indicates charge transfer limitations and its diameter is equals to charge transfer resistance (R_{ct}) and second part of Nyquist plot is straight line appears in low frequencies indicates mass transfer limitations. The Zview software was used for fitting and simulation of EIS data and also randles equivalent circuit which was illustrated in the inset of Fig. 2 was selected as equivalent circuit for fitting and simulation of EIS data. The R_{ct} values of GCE/MWCNTs-CH, GCE/GP-CH, GCE/BB-CH, GCE/G-CH and GCE/CH were obtained 0.38, 0.45, 1.1, 17 and 21 Ω , respectively. The R_{ct} of electrodes increases from GCE/MWCNTs-CH to GCE/CH. The remarkable decrease in R_{ct} of GCE/MWCNT-CH < GCE/GP-CH < GCE/BB-CH, compare to others modifier is due to presence of MWCNTs, GP and BB with high conductivity of the mentioned modifiers in the modified electrodes.

3.3. Electrochemical characterization of the electrodes

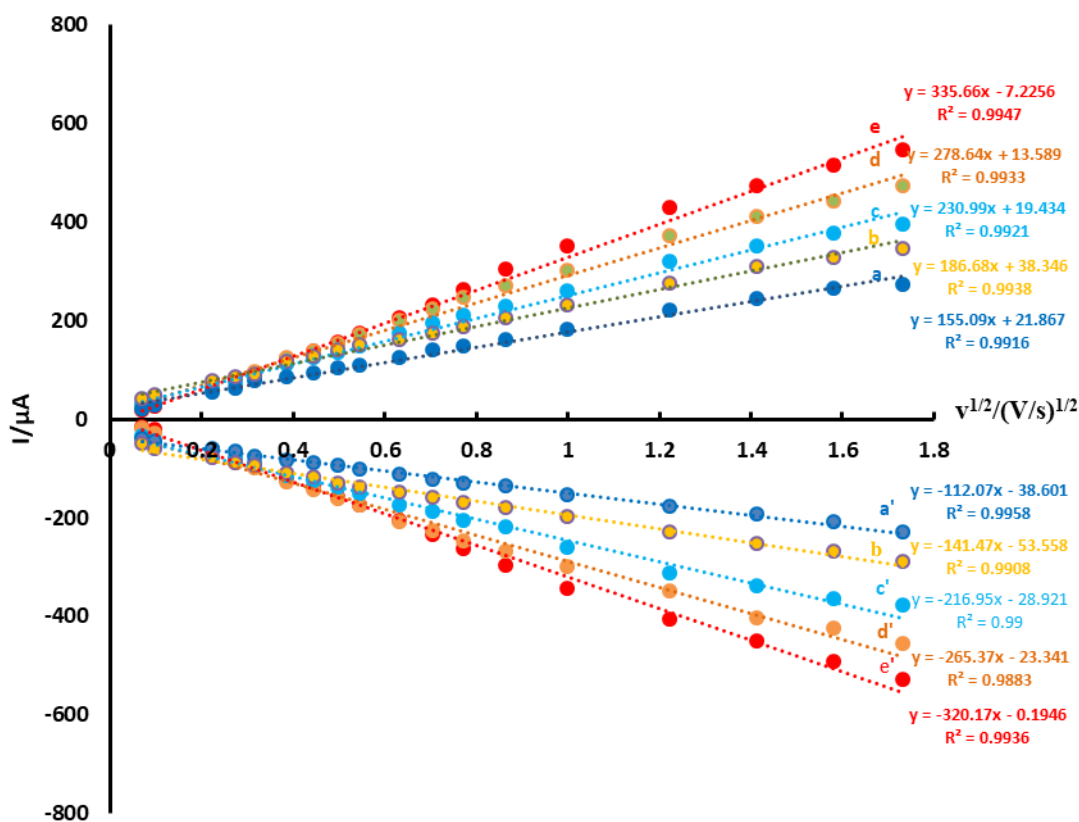


Figure 3. The plot of I_{pa} and I_{pc} vs. $v^{1/2}$ for (a, a') GCE/CH (b, b') GCE/G-CH (c, c') GCE/BB-CH (d, d') GCE/GP-CH and (e, e') GCE/MWCNTs/CH.

Electrochemical measurements of the GCE/MWCNTs-CH, GCE/GP-CH, GCE/BB-CH, GCE/G-CH and GCE/CH were analyzed for the anodic peak current (I_{pa}) of the respective cyclic voltammograms obtained in the presence of 1.0 mM of $Fe(CN)_6^{3-/4-}$ in KCl 0.1 M as supporting

electrolyte (not shown). All assays were performed by cyclic voltammetry in the potentials ranges of -0.5 to 1.2 V as a probe at different scan rates. Figure 3 was shown the anodic and cathodic peak currents vs. the square root of scan rate of the $\text{Fe}(\text{CN})_6^{3-/4-}$. For a reversible process, the Randles–Sevcik equation can be used as follow [21]:

$$I_{pa} = 2.69 \times 10^5 n^{3/2} A C_0 D_R^{1/2} \nu^{1/2} \quad (1)$$

In this equation I_{pa} , n , A , D_R , C_0 and ν refer to the anodic peak current, the electron transfer number, the surface area of the electrode, the diffusion coefficient, the concentration of $\text{Fe}(\text{CN})_6^{3-/4-}$ and the scan rate, respectively. For 1mM $\text{Fe}(\text{CN})_6^{3-/4-}$ in the 0.1M KCl electrolyte, $n = 1$ and $D_R = 7.6 \times 10^{-6} \text{ cm}^2 \text{ s}^{-1}$ [22], the microscopic areas were calculated from the slope of the I_{pa} vs. $\nu^{1/2}$ relation. The calculated electrode surface for the GCE/MWCNTs–CH, GCE/GP-CH, GCE/BB-CH, GCE/G-CH and GCE/CH were found to be 0.453, 0.375, 0.311, 0.258 and 0.209 cm^2 , respectively. Therefore, the results indicated that the presence of CNTs greatly improved the effective area of the electrode and contribute to an increase in the conductivity of the sensor.

3.4. Electrochemical behavior of AA, EP, UA, NO_2^- and XN at different electrodes

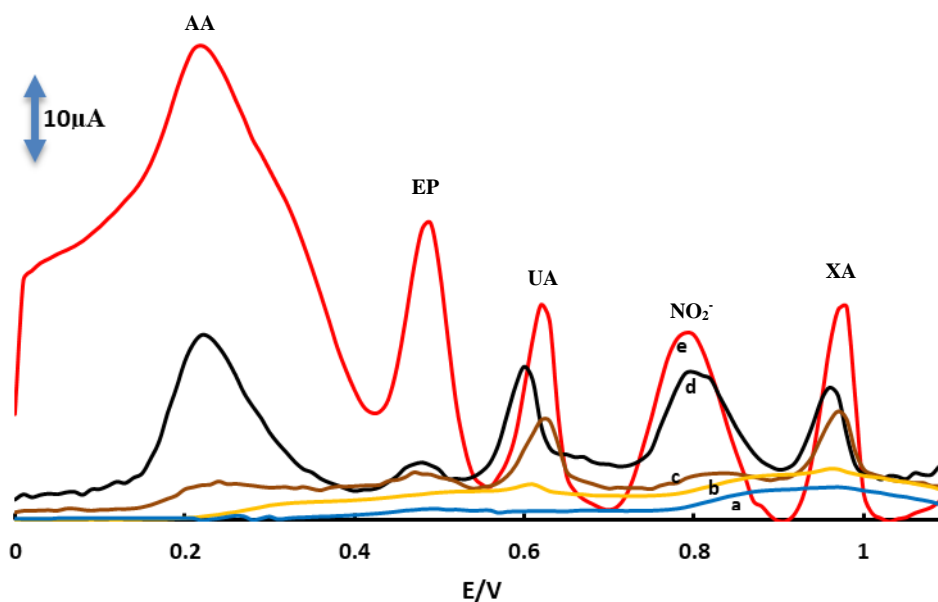


Figure 4. DPVs in pH=2 PBS in Presence mix AA, EP, UA, NO_2^- , XN analytes for (a) GCE/CH (b) GCE/G-CH (c) GCE/BB-CH (d) GCE/GP-CH and (e) GCE/MWCNTs/CH.

Fig. 4 shows the differential pulse voltammetry (DPV) of a mixture of 3.125 mM AA, 82.5 μM EP, 21 μM UA, 1.25 mM NO_2^- and 21 μM XN at the surface of GCE/MWCNTs–CH, GCE/GP-CH, GCE/BB-CH, GCE/G-CH and GCE/CH in a 0.1 M PBS with pH=2 at scan rate of 50 mVs^{-1} . As shown in Fig. 4a, there are not any oxidation peaks for AA, EP, UA, NO_2^- and XN on the surface of GCE/CH but there are a weak peak for UA at potential 0.61 V and a merge and weak peak for the NO_2^- and XN at potential 0.96 V on the surface of GCE/G-CH (Fig. 4b) and there are not any acceptable peaks for the other compounds. The GCE/BB-CH shows five weak peaks for AA, EP, UA,

NO_2^- and XN at potential 0.22, 0.45, 0.63, 0.82 and 0.98 V, respectively (Fig. 4c). Based on Fig. 4d and 4e, the oxidation peaks of AA, EP, UA, NO_2^- and XN have been separated with a considerable enhancement in the anodic peak current for AA, EP, UA, NO_2^- and XN by using of the GP and MWCNTs as modifiers of the GCEs. These results indicated the five well separated and significant enough anodic peak currents, corresponding to oxidation of AA, EP, UA, NO_2^- and XN on the GCE/MWCNTs-CH to apply for accurate, sensitive and simultaneous determination of AA, EP, UA, NO_2^- and XN in different samples.

3.5. Influence of pH on the simultaneous oxidation of AA, EP, UA, NO_2^- and XN

The effect of solution pH on the electrochemical response of the GCE/MWCNTs-CH toward the simultaneous oxidation of AA, EP, UA, NO_2^- and XN was also studied. Fig. 5A shows the DPVs of AA, EP, UA, NO_2^- and XN at various pH levels. Based on these results, pH 2 exhibits the best peak separation and highest peak current for the GCE/MWCNTs-CH and this pH was chosen as optimum pH. Also, it was found that the anodic peak potentials for AA, EP, UA, NO_2^- and XN shifted to negative potentials when the pH increased. This was expected, due to the participation of proton(s) in the oxidation reactions of AA, EP, UA, NO_2^- and XN. The results represented in Fig. 5B, shows that the anodic potential shifts toward negative values with increasing the pH. The equations 2-6 show the relationship between E_p of the AA, EP, UA, NO_2^- and XN and pH.

$$E_p(\text{AA}) = -0.0623\text{pH} + 0.3423 \quad R^2 = 0.9791 \quad (2)$$

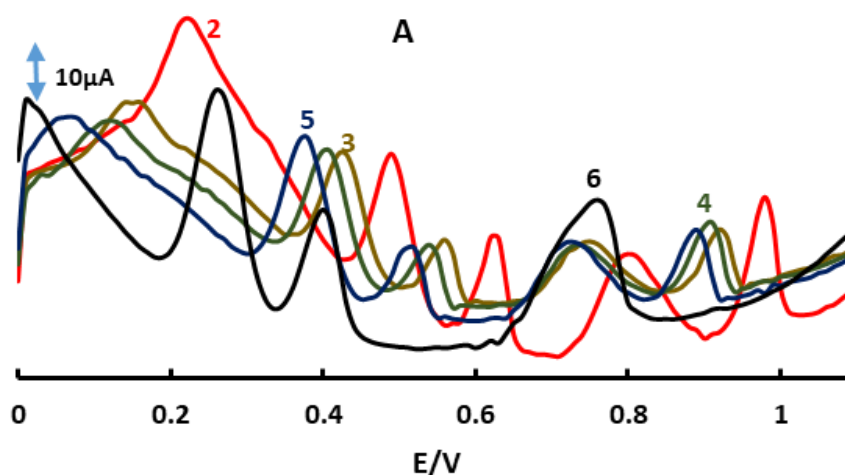
$$E_p(\text{EP}) = -0.0636\text{pH} + 0.6111, \quad R^2 = 0.9939 \quad (3)$$

$$E_p(\text{UA}) = -0.0596\text{pH} + 0.7416 \quad R^2 = 0.9892 \quad (4)$$

$$E_p(\text{NO}_2^-) = -0.0279\text{pH} + 0.8524 \quad R^2 = 0.9661 \quad (5)$$

$$E_p(\text{XN}) = -0.0479\text{pH} + 1.0659 \quad R^2 = 0.9786 \quad (6)$$

As anticipated, these equations advocate compromising of theoretical slope of $(-\frac{2.303mRT}{nF})$ of $0.059(\frac{m}{n})\text{V}$ and rising of pH (where, m and n are the number of protons and electrons involved in the reaction). These results express the equality in the number of protons and electrons that are involved in the processes of AA, EP, UA, NO_2^- and XN.



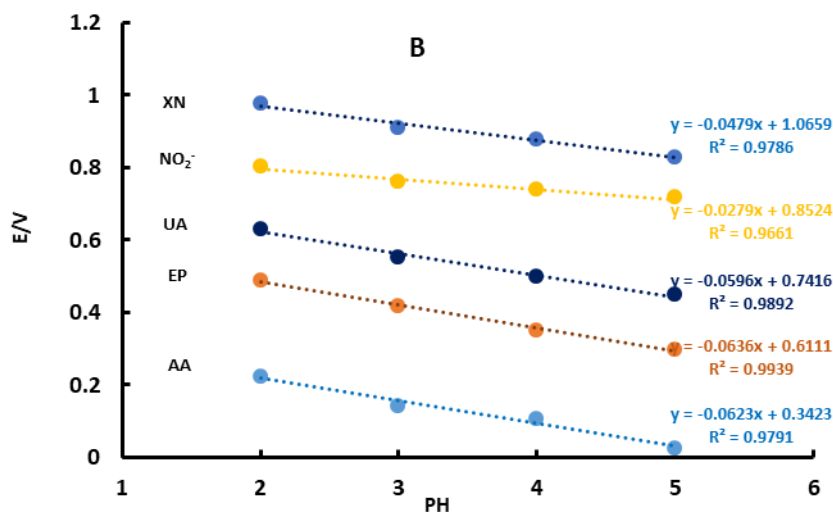
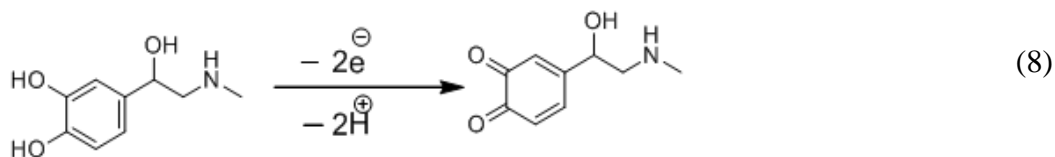
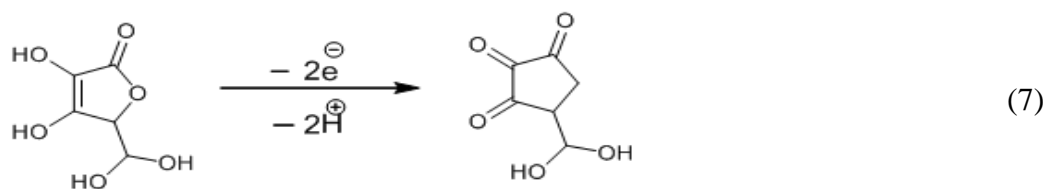


Figure 5. (A) DPVs of the GCE/MWCNTs-CH of 3.125 mM AA, 82.5 μM EP, 21 μM UA, 1.25 mM NO₂⁻, 21 μM XN at scan rate of 50 mVs⁻¹ with pH values 2 to 6 (B) Variation of E_p versus the various buffered pH values: 2, 3, 4, and 5.

As can be seen from Fig. 6B, the E_{p(red)} values were shifted to negative potentials with slopes of 0.0623, 0.0636, 0.096, 0.0279 and 0.0479V *per* pH for AA, EP, UA, NO₂⁻ and XN, respectively. AA, EP, UA, and XN are in agreement with the theoretical slope of 0.059 (m/n)V per pH. These results suggest that the oxidation of AA, EP, UA and XN involves an equal number of protons and electrons (m=n). This conclusion is in accordance with the known electrochemical reactions of AA, EP, UA, and XN at the surface of GCE/MWCNTs-CH, which are illustrated in eqs. (7)-(10) and for NO₂⁻ slope 0.0279 in agreement with the theoretical slope 0.028 (m/n)V per pH. This result suggest that the oxidation of NO₂⁻ involves an unequal number of protons and electrons (m≠n), the ratio of the number of electrons to protons is 2 to 1. An electrochemical reaction of NO₂⁻ at the surface of GCE/MWCNTs-CH is illustrated in eq. (11).



3.6. Effect of scan rate

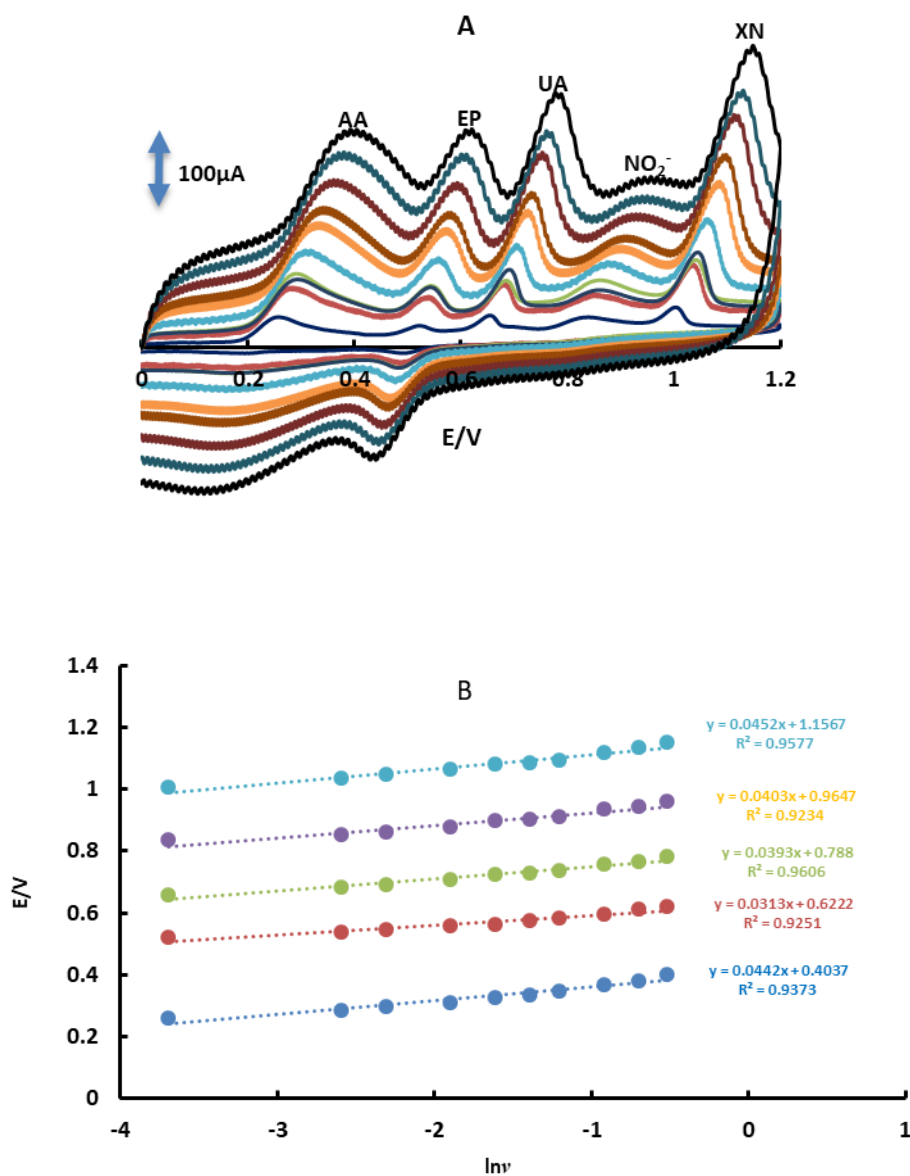


Figure 7. (A) CVs of the GCE/MWCNTs-CH in the presence of 3.125 mM AA, 82.5 μM EP, 21 μM UA, 1.25 mM NO₂⁻, 21 μM XN in pH=2 PBS at various scan rates: 25, 75, 100, 150, 200, 250, 300, 400, 500 and 600 mVs⁻¹ (B) Variation of the potential peaks versus ln v

The effect of scan rate on the electrochemical oxidation of AA, EP, UA, NO₂⁻ and XN at the GCE/MWCNTs-CH was investigated by CV (Fig. 7A). The oxidation peak potentials for AA, EP, UA, NO₂⁻ and XN shifted to more positive values with increasing scan rate, confirming the kinetic limitations of the electrochemical reaction. This shows that the oxidation of AA, EP, UA, NO₂⁻ and XN are an irreversible charge transfer process. The plot of E_p and ln(v) (see Fig. 7B) was a straight line with a slope [24]:

$$\frac{\delta E_p}{\delta (\ln v)} = \frac{RT}{(1-\alpha)nF} \tag{12}$$

where α stands for the electron transfer coefficient, the slope of E_p vs. $\ln(v)$. Plot for AA, EP, UA, NO_2^- and XN were 0.044, 0.031, 0.039, 0.040 and 0.045 V, respectively. The α values for $n=2$ and $T=298$ K were calculated as 0.71, 0.59, 0.67, 0.68 and 0.71 for AA, EP, UA, NO_2^- and XN.

3.7. Chronoamperometric measurements

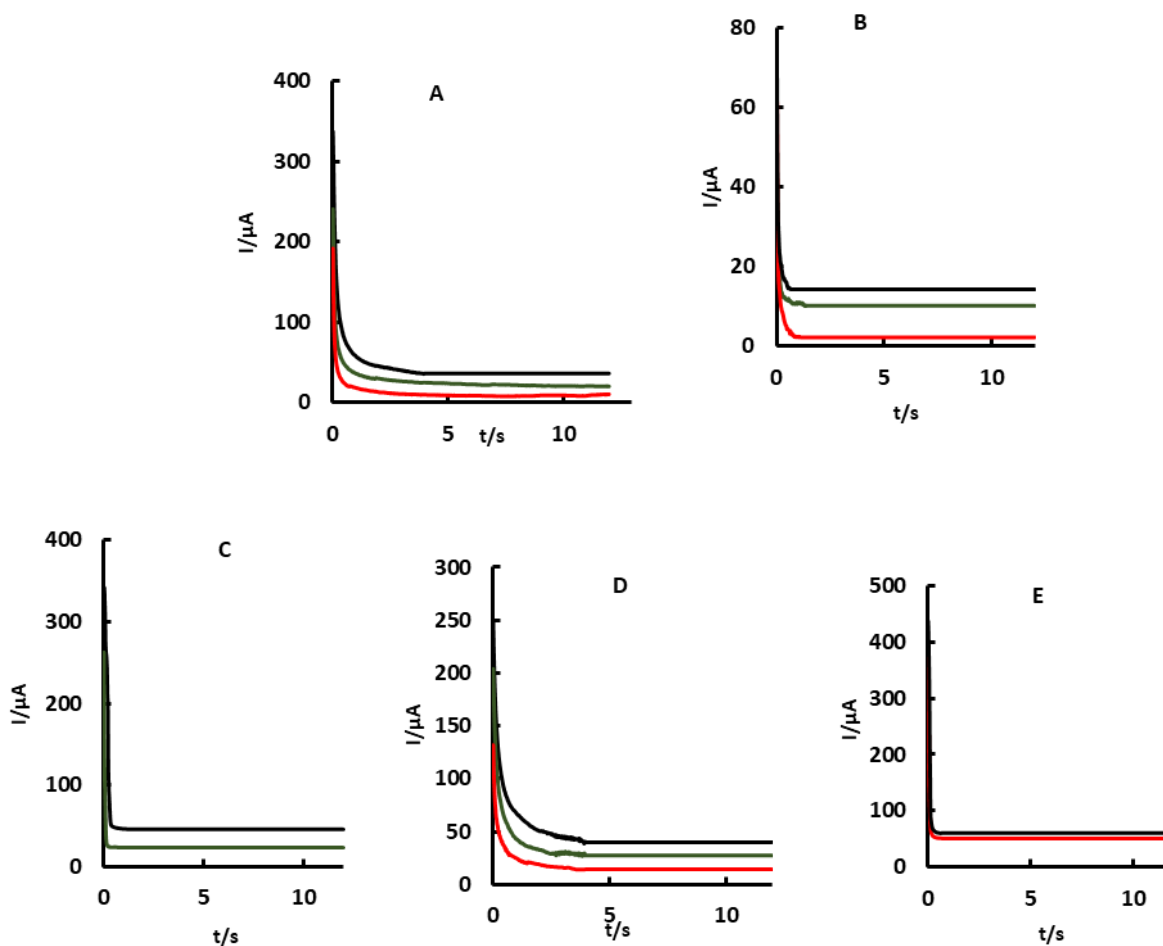


Figure 8. Chronoamperograms obtained at the GCE/MWCNTs-CH in 0.1 M PBS (pH=2) (A) for different concentrations of AA: 1.3, 2.6, 7.8 mM. (B) for different concentrations of EP: 0.13, 0.26 μM (C) for different concentrations of UA: 0.03, 0.06 μM (D) for different concentrations of NO_2^- : 0.66, 1.3, 1.96 mM. (E) for different concentrations of XN: 0.016, 0.033 μM

Chronoamperometric method of AA, EP, UA, NO_2^- and XN at the GCE/MWCNTs-CH were carried out by setting the working electrode potentials at 0.29, 0.54, 0.68, 0.85 and 1.04 V, respectively. At the first potential step vs. Ag/AgCl for various concentrations of AA, EP, UA, NO_2^- and XN in PBS (pH=2) singly; as presented in Fig. 8, for electroactive materials (AA, EP, UA, NO_2^- and XN) with a diffusion coefficient D , the current observed for the electrochemical reaction under mass transport-limited conditions can be described by the Cottrell equation[25]:

$$I = n F A D^{1/2} C \pi^{-1/2} t^{-1/2} \tag{13}$$

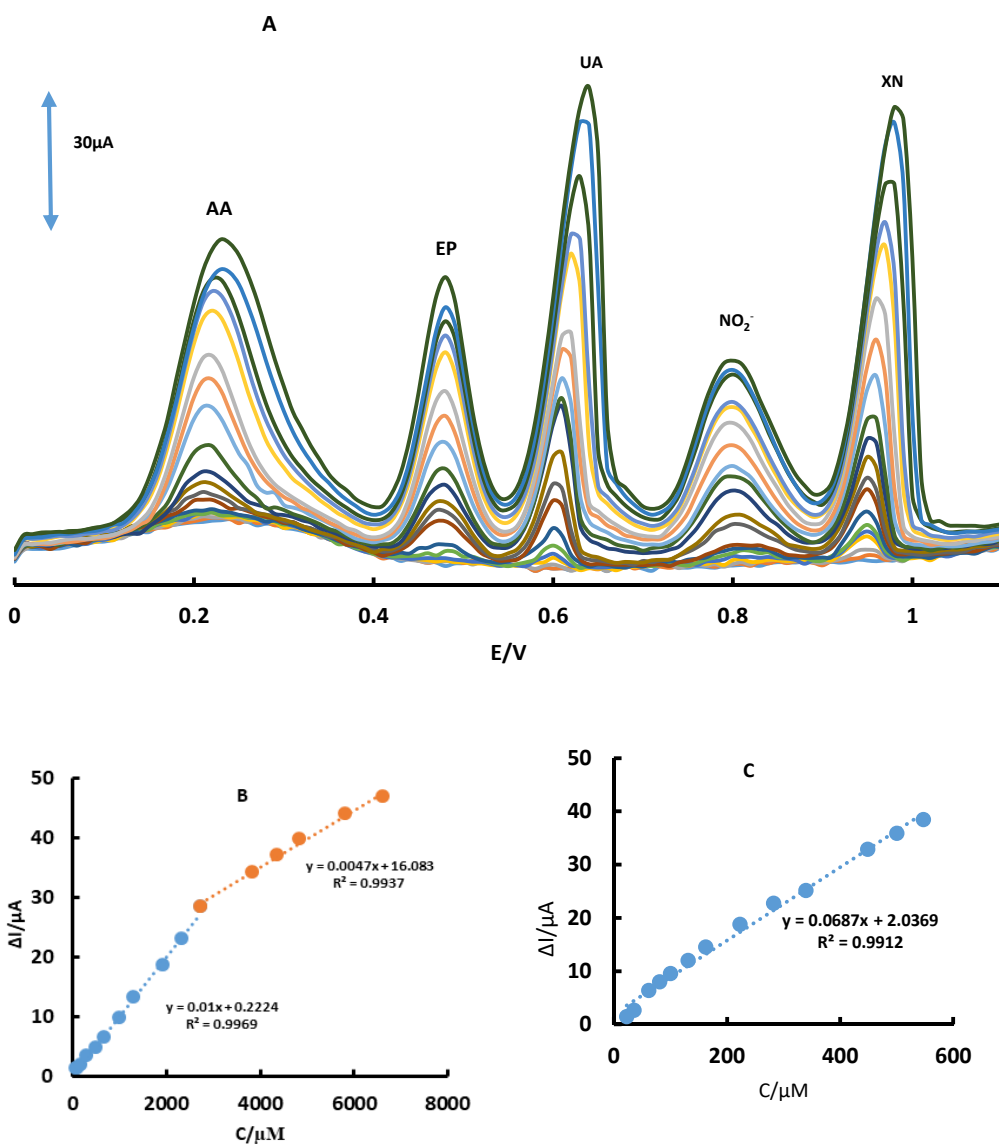
The values of the diffusion coefficient (D) were found to be 6.97×10^{-6} , 3.5×10^{-5} , 1.3×10^{-4} , 4.7×10^{-5} and 6.9×10^{-4} $\text{cm}^2 \text{s}^{-1}$, for AA, EP, UA, NO_2^- and XN.

The standard heterogeneous rate constant (K_s) for the electrochemical reactions AA, EP, UA, NO_2^- and XN at the surface of the GCE/MWCNTs-CH, can be evaluated by CVs according to using the Velasco equation, as given below[26]:

$$K_s = 1.11 D_0^{1/2} (E_P - E_{P1/2})^{-1/2} v^{1/2} \tag{14}$$

where K_s refers to The standard heterogeneous rate constant, D_0 is the diffusion coefficient, E_P and $E_{P1/2}$ refer to potential peak and potential in half of peak currents, respectively, and v is scan rate. the values of The standard heterogeneous rate constant (K_s) were found to be 5.21×10^{-3} , 1×10^{-2} , 2.3×10^{-2} , 1.2×10^{-2} and 5.6×10^{-2} cm s^{-1} for AA, EP, UA, NO_2^- and XN, respectively.

3.8. Linear range, detection limit and simultaneous determination and interference study



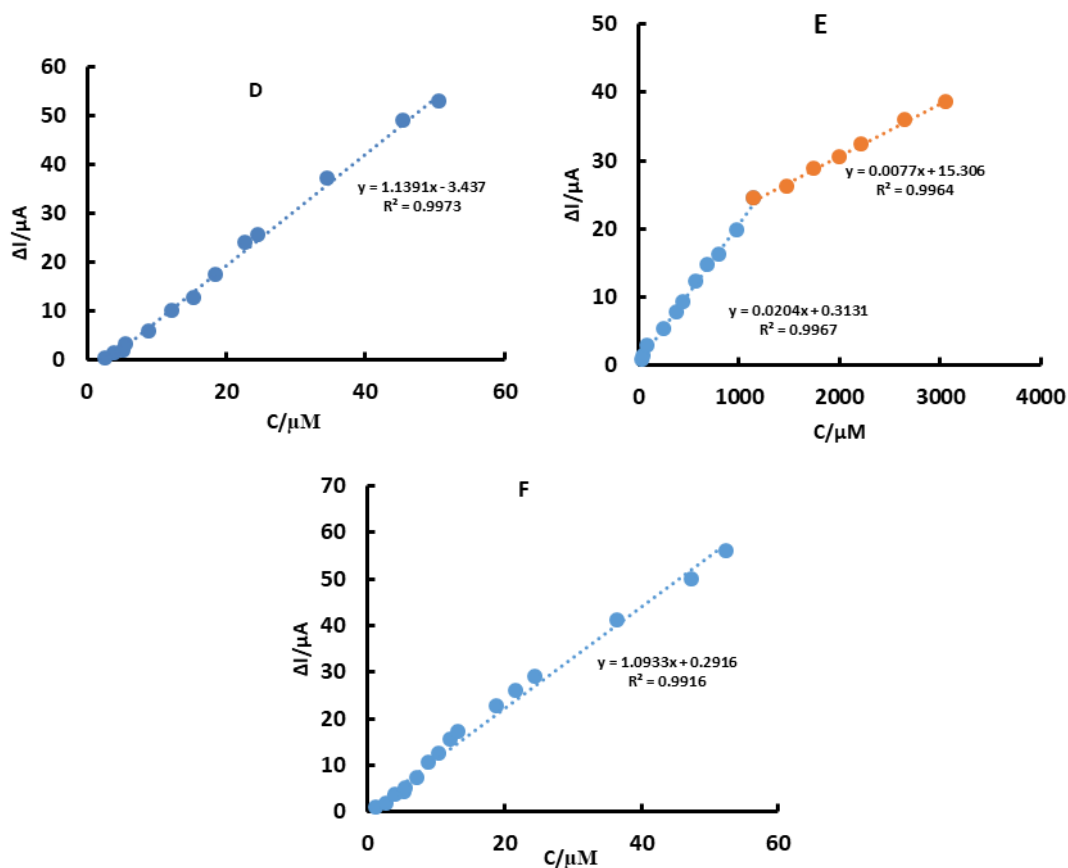


Figure 9. (A) DPVs of the GCE/MWCNTs-CH in 0.1 M PBS (pH=2) containing different concentrations of AA, EP, UA, NO_2^- and XN. plots of ΔI_p vs. concentration (B) AA (C) EP (D) UA (E) NO_2^- and (F) XN.

DPV was used for simultaneous determination of AA, EP, UA, NO_2^- and XN on the GCE/MWCNTs-CH (Fig. 9A). In order to obtain the best sensitivity under the specific conditions, an amplitude scan rate of 50 mVs^{-1} and pH=2 were selected.

The responses were linear with AA concentration consisted of two linear segments with slopes of 0.01 and $0.0047 \mu\text{A } \mu\text{M}^{-1}$ in the concentration ranges from $53.1 \mu\text{M}$ to 2.32 mM and 2.32 mM to 6.61 mM , respectively (see Fig. 9B). The dynamic range for EP was linear in the range from $22.5 \mu\text{M}$ to $547 \mu\text{M}$ and the current sensitivity was $0.0687 \mu\text{A } \mu\text{M}^{-1}$ (see Fig. 9C). The responses were linear with UA concentration in the range from $2.66 \mu\text{M}$ to $50.6 \mu\text{M}$ and the current sensitivity was $1.1391 \mu\text{A } \mu\text{M}^{-1}$ (see Fig 9D). The plot of peak current vs. NO_2^- concentration consisted of two linear segments with slopes of 0.0204 and $0.0077 \mu\text{A } \mu\text{M}^{-1}$ in the concentration ranges from $39.9 \mu\text{M}$ to 1.15 mM and 1.15 mM to 3.05 mM , respectively (see Fig. 9E). The decrease in sensitivity (slope) of the second linear segment for AA and NO_2^- are likely due to kinetic limitation. Finally, the dynamic range was linear with XN concentration in the range from $1.33 \mu\text{M}$ to $52.4 \mu\text{M}$ and the current sensitivity was $1.0933 \mu\text{A } \mu\text{M}^{-1}$ (see Fig. 9F). The detection limits were determined to be 16.3, 3.92, 0.37, 29.9 and $0.13 \mu\text{M}$ for AA, EP, UA, NO_2^- and XN (based on $Y_{\text{LOD}} = Y_{\text{B}} + 3\delta$).

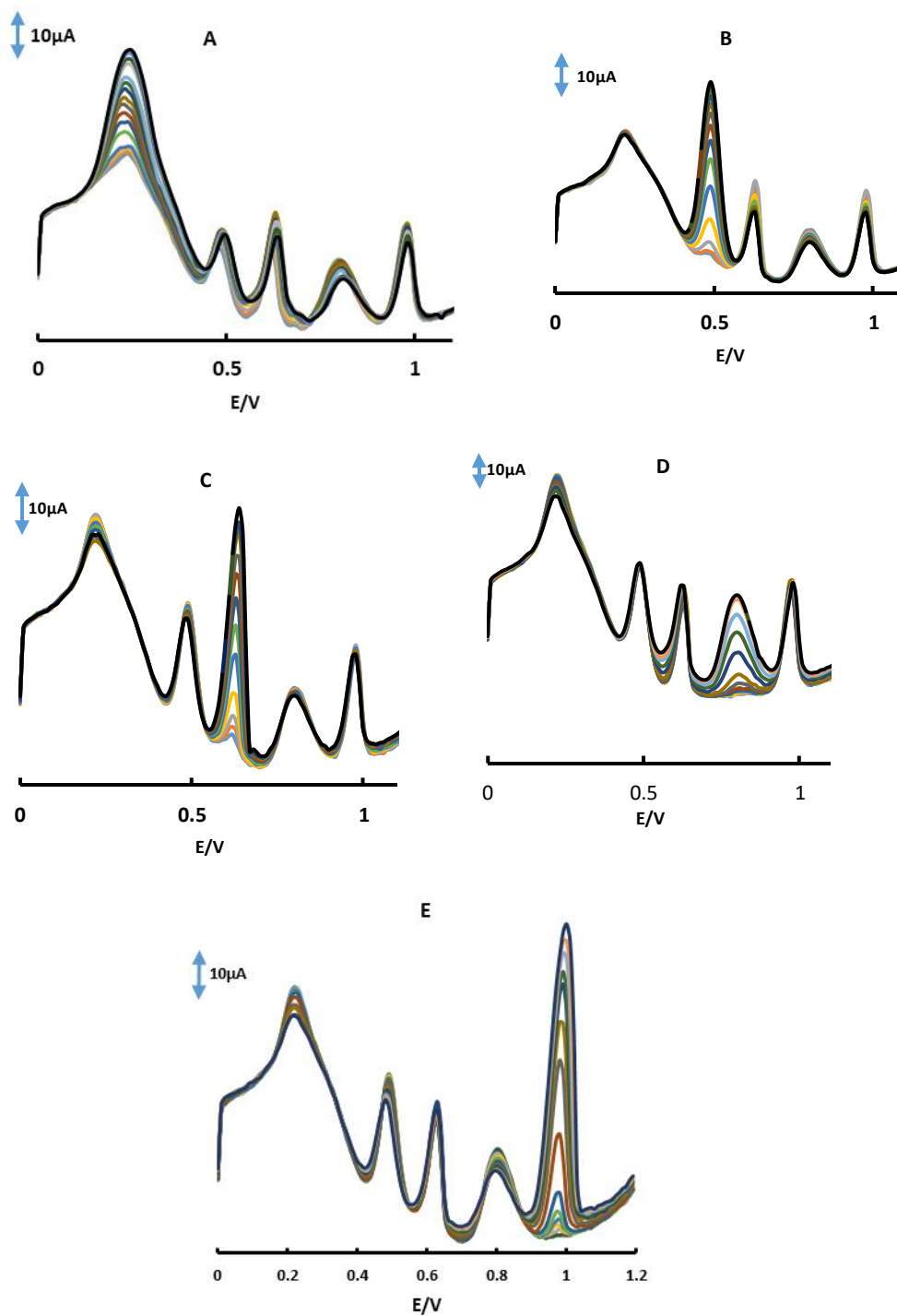


Figure 10. DPVs at the GCE/MWCNTs-CH in 0.1 M PBS (pH=2) (A) containing EP (0.64mM), UA (0.64 mM), NO_2^- (1.29 μM) and XN (0.45 μM) and different concentrations of AA (B) Containing AA (3.15 μM), UA (0.63 mM), NO_2^- (1.26 μM) and XN (0.44 μM) and different concentrations of EP (C) Containing AA (3.15 μM), EP (0.63 mM), NO_2^- (1.26 μM) and XN (0.44 μM) and different concentrations of UA (D) Containing AA (3.17 μM), EP (0.63 μM), UA (0.63 μM) and XN (0.44 μM) and different concentrations of NO_2^- (E) Containing AA (3.14 μM), EP (0.62 μM), UA (0.62 mM) and NO_2^- (1.25 μM) and different concentrations of XN.

In the simultaneous determination, it is very important to study the interferences of each other for the selective detection of one species. In each experiment, the concentration of one species changed, while the concentrations of the other one were kept constant. The results are shown in Fig. 10.

It can be seen from Fig. 10 that the peak current of AA increases with an increase in the concentration of AA, while the peak current for the oxidation of EP, UA, NO_2^- and XN remain constant. As it can be seen the voltammetric peak corresponding to the oxidation of EP, UA, NO_2^- and XN were found to increase linearly in consonance with the increase in their concentrate EP, UA, NO_2^- and XN, whereas the peak current for the oxidation of other four compounds remain constant. The results showed that the peak currents are linearly proportional to the concentrations of AA (or EP, UA, NO_2^- and XN) while those of the other compounds did not changed; indicating that the oxidation of AA, EP, UA, NO_2^- and XN at GCE/MWCNTs-CH takes place independently.

3.9. Analytical application

The applicability of the GCE/MWCNTs-CH was examined for the simultaneous determination of AA, EP, UA, NO_2^- and XN in human serum, urine samples and vitamin C tablets. The DPV were obtained by spiking appropriate samples in diluted solution using the GCE/MWCNTs-CH under the optimum conditions, as described earlier. The results were shown in Tables 1–3 for human urine and surum as well as AA tablets, respectively. As evidenced in these tables, acceptable recovery values were obtained, which point to the applicability of this modified electrode for trace amounts of these compounds in the real sample analysis. Furthermore, the human urine samples were also analyzed with standard methods [27, 28]. Based on the results in Table 1, there are good agreements with the results obtained with the proposed method and standard methods for AA, EP, UA, XN and NO_2^- . Based on the results in these tables, the proposed methods could be efficiently used for the determination of trace amounts of these compounds in biological systems and pharmaceutical preparations.

Table 1. Determination of AA, EP, UA, NO_2^- and XN in urine sample at pH 2 (n=3)

Samples	AA (μM)		EP (μM)		UA (μM)		NO_2^- (μM)		XN (μM)	
	PM ^a	SM ^b [27]	PM	SM[27]	PM	ST[27]	PM	SM[28]	PM	SM[27]
Human urine	-	-	-	-	14.8	-	7.4	-	3.2	-
Added	100.0	-	100.0	-	10.0	-	100.0	-	10.0	-
Found	98.6	101.5	100.05	112.0	10.09	10.3	97.2	104.5	10.13	9.87
Recovery (%)	98.6	101.5	100.05	112.0	100.9	103.0	97.2	104.5	101.3	98.7
RSD (%)	1.3	1.8	1.5	2.0	1.9	1.6	2.1	2.8	1.1	2.2
Added	200.0	--	200.0	-	20.0	-	200.0	-	20.0	-
Found	200.2	195.9	195.2	197.0	19.4	20.7	207.5	195.7	21.1	20.5
Recovery (%)	100.1	98.0	97.6	98.5	97.0	103.5	103.8	97.9	105.5	102.5
RSD (%)	2.4	2.1	1.2	1.7	2.6	2.1	1.7	1.9	1.9	2.2
Added	300	-	300	-	30	-	250	-	30.0	-
Found	297.3	290.4	300.47	294.3	29.2	31.0	255.2	259.5	31.5	29.4
Recovery (%)	99.1	103.2	100.2	98.1	97.3	103.3	102.1	103.8	105.0	98.0
RSD (%)	2.8	1.9	2.3	1.7	2.9	2.1	2.7	1.8	1.7	2.2

^aProposed method

^bStandard method

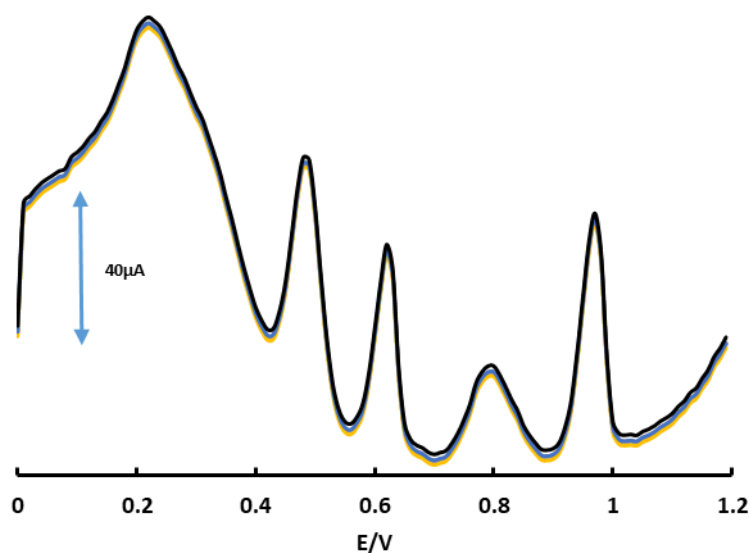
Table 2. Determination of AA, EP, UA, NO₂⁻ and XN in human serum at pH 2 (n=3)

Samples	AA (μM)	EP (μM)	UA (μM)	NO ₂ ⁻ (μM)	XN (μM)
human blood serum	-	-	7.8	-	3.1
Added	100	100	10	100	10
Found	100.2	100.4	17.5	100.1	13.2
Recovery (%)	100.2	100.4	97	100.1	101
RSD (%)	1.9	2.1	1.5	1.8	1.3
Added	200	200	20	200	20
Found	199.1	199.2	27.93	197.5	22.94
Recovery (%)	99.55	99.6	100.65	98.75	99.2
RSD (%)	2.1	1.5	1.3	2.1	1.9
Added	300	300	30	250	30
Found	297.6	300.14	37.95	249	33.3
Recovery (%)	99.2	100.04	100.5	99.6	100.66
RSD(%)	3.1	1.9	1.7	2.4	1.1

Table 3. Determination of AA, EP, UA, NO₂⁻ and XN in AA tablets at pH 2 (n=3)

Samples	AA (μM)	EP (μM)	UA (μM)	NO ₂ ⁻ (μM)	XN (μM)
AA tablet	20	-	-	-	-
Added	-	100	10	100	10
Found	19.7	99.8	10.3	97.8	10.21
Recovery (%)	98.5	99.8	103	97.8	102.1
RSD (%)	2.7	1.6	1.9	3.1	2.1
AA tablet	50	-	-	-	-
Added	-	200	20	200	20
Found	51.41	207.3	20.9	197.9	20.3
Recovery (%)	102.82	103.65	104.5	98.95	101.5
RSD (%)	2.4	1.7	1.1	2.3	1.8

3.10. Stability and reproducibility



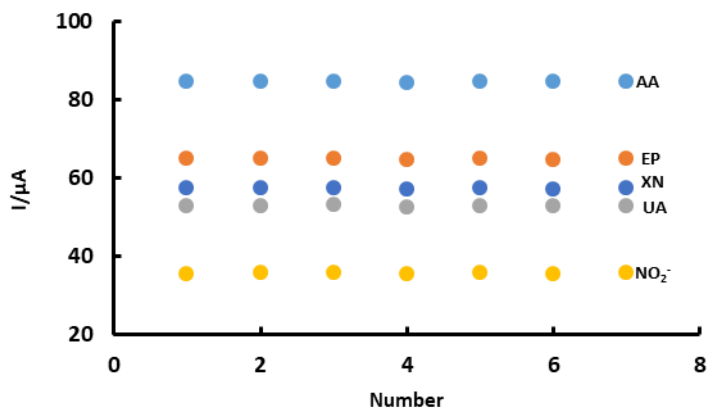


Figure 11. The stability of repetitive measurements of DPV response of GCE/MWCNTs-CH for 3.125 μM AA, 82.5 μM EP, 21 μM UA, 1.25 mM NO_2^- and 21 μM XN in 0.1M PBS (pH=2) at scan rates 50 mVs^{-1} .

The stability and reproducibility of the GCE/MWCNTs-CH modified electrode were investigated. DPVs for a mixture of AA (3.125 μM), EP (82.5 μM), UA (21 μM), NO_2^- (1.25 mM) and XN (21 μM) in 0.1 M PBS (pH=2.) at GCE/CNTs-CH electrode was shown in Fig. 11.

Based on the result, the electrochemical signals of analytes on the GCE/MWCNTs-CH electrode have an excellent stability and reproducibility.

4. CONCLUSIONS

In this work, we compared the electrochemical behavior of the different modified GCE with MWCNTs, GP, BB and G for the simultaneous determination of AA, EP, UA, NO_2^- and XN. The GCE/MWCNTs-CH showed the most surface area, the best separation peaks and enhanced the oxidation peak currents and excellent selectivity for simultaneous determination of AA, EP, UA, NO_2^- and XN. The results showed a wide linear concentration range and low detection limits for the analytes. In addition, this proposed method can be applied to the determination of AA, EP, UA, NO_2^- and XN in real samples with satisfactory results.

ACKNOWLEDGEMENTS

We gratefully acknowledge the financial support of the University of Sistan and Baluchestan.

References

1. A. McNaught and A. McNaught, *Compendium of chemical terminology*, Blackwell Science Oxford; 1997.
2. Y. Pan, M. Hu, M. Ma, Z. Li, Y. Gao, M. Xiong, G. Gao, Z. Zhao, Y. Tian, B. Xu and J. He, *Carbon*, 115 (2017) 584.
3. N. Yahya, *Carbon and oxide nanostructures*, Springer; 2011.
4. A. Hirsch, *Nat. Mater.*, 9 (2010) 868.

5. A. Sulong, M. Ramli, S. Hau, J. Sahari, N. Muhamad and H. Suherman. *Composites Part B*. 50 (2013) 54.
6. M. Noroozifar, M. Khorasani Motlagh, R. Akbari and M. Bemanadi Parizi. *Anal. Bioanal. Chem. Research*, 1 (2014) 62.
7. M. Moghadam, S. Dadfarnia, A. Shabani and P. Shahbazikhah, *Anal. Biochem.*, 410(2) (2011) 289.
8. A. Florou, M. Prodromidis, M. Karayannis and S. Tzouwara-Karayanni, *Anal. Chim. Acta*, 409 (2000) 113.
9. M. Davies, J. Austin and D. Partridge, *Vitamin C: its chemistry and biochemistry: royal society of chemistry*, 1991.
10. Y. Zeng, J. Yang and K. Wu, *Electrochim. Acta*, 53 (2008) 4615.
11. S. Shahrokhian, M. Ghalkhani and M. Amini, *Sens. Actuator B-Chem.*, 137 (2009) 669.
12. G. Guilbault, *Marcel Dekker Inc*, 1984.
13. D. Branson, *Tech. Bull. Regist. Med. Technol.*, 36 (1966) 288.
14. M. Gladwin, J. Shelhamer, A. Schechter, M. Pease-Fye, M. Waclawiw, J. Panza, F. Ognibene and R. Cannon, *Proc. Natl. Acad. Sci.*, 97 (2000) 11482.
15. D. Metzler, *Biochemistry: the chemical reactions of living cells*, Academic Press; 2003.
16. Y. Sun, J. Fei, K. Wu and S. Hu, *Anal. Bioanal. Chem.*, 375 (2003) 544.
17. X. Tang, Y. Liu, H. Hou and T. You, *Talanta*, 83 (2011) 1410.
18. X. Liu, W. Lin, X. Yan, X. Chen, J. Hoidal and P. Xu, *J. Chromatogr. B*, 785 (2003) 101.
19. S. Bas, E. Maltas, B. Sennik and F. Yilmaz, *Colloids. Surf. A: Physicochem. Eng. Asp.*, 444 (2014) 40.
20. S. Hu and C. Liu, *Electroanalysis*, 9 (1997) 372.
21. V. Gau, S. Ma, H. Wang, J. Tsukuda, J. Kibler and D. Haake. *Methods*, 37 (2005) 73.
22. H. Rajabi, M. Noroozifar and M. Khorasani-Motlagh, *Anal. Methods*, 8(8) (2016) 1924.
23. M. Mehdi Foroughi, · M. Noroozifar and M. Khorasani-Motlagh, *J. Iran. Chem. Soc.*, 12 (2015) 1139.
24. H. Tong, H. Li and X. Zhang, *Carbon*, 45 (2007) 2424.
25. A. Bard and L. Faulkner, *Fundamentals and applications. Electrochemical Methods*, 2nd ed, Wiley: New York, 2001.
26. J. Velasco, *Electroanalysis*, 9 (1997) 880.
27. S. Zhou, R. Zuo, Z. Zhu, D. Wu, K. Vasa, Y. Deng and Y. Zuo, *Anal. Methods*, 5 (2013) 1307.
28. F. Rincón, B. Martínez and J. Delgado, *Meat Sci.*, 65 (2003) 142